Hindawi
Journal of Spectroscopy
Volume 2020, Article ID 8137142, 10 pages
https://doi.org/10.1155/2020/8137142

Research Article

Study on the Calibration Transfer of Soil Nutrient Concentration from the Hyperspectral Camera to the Normal Spectrometer

Xue-Ying Li,[1,2,3] Guo-xing Ren,[1,2,3,4] Ping-Ping Fan,[1,2,3] Yan Liu,[1,2,3] Zhong-Liang Sun,[1,2,3] Guang-Li Hou,[1,2,3] and Mei-Rong Lv[1,2,3]

[1]*Institute of Oceanographic Instrumentation, Qilu University of Technology (Shandong Academy of Sciences), Qingdao, China*
[2]*Shandong Provincial Key Laboratory of Ocean Environmental Monitoring Technology, Qingdao, China*
[3]*National Engineering and Technological Research Center of Marine Monitoring Equipment, Qingdao, China*
[4]*Department of Information Science and Engineering, Ocean University of China, Qingdao, China*

Correspondence should be addressed to Mei-Rong Lv; 444868063@qq.com

Received 28 April 2019; Accepted 24 March 2020; Published 27 April 2020

Academic Editor: Pedro D. Vaz

The calibration transfer between instruments is mainly aimed at the calibration transfer between normal spectrometers. There are few studies on the calibration transfer of soil nutrient concentration from a hyperspectral camera to a normal spectrometer. In this paper, 164 soil samples from three regions in Qingdao, China, were collected. The spectral data of normal spectrometer and hyperspectral camera and the concentration of total carbon and nitrogen were obtained. And then, the models of soil total carbon and nitrogen content were established by using the spectral data of a normal spectrometer. The hyperspectral data were transferred by a variety of methods, such as single conventional calibration transfer algorithm, combination of multiple calibration transfer algorithms, and calibration transfer algorithm after spectral pretreatment. The transferred hyperspectral data were predicted by the total carbon and total nitrogen concentration model established by using a normal spectrometer. The absolute coefficients R_t^2 and root mean square error of prediction (RMSEP) were used to evaluate the prediction performance after calibration transfer. After trying many calibration transfer methods, the prediction performance of calibration transfer by the Repfile-PDS and Repfile-SNV methods was the best. In the calibration transfer of the Repfile-PDS method, when the number of PDS windows was 27 and the number of standard data was 40, the R_t^2 and the RMSEP of TC concentration were 0.627 and 2.351. When the number of PDS windows was 25 and the number of standard data was 100, the R_t^2 and the RMSEP of TN concentration were 0.666 and 0.297. In the calibration transfer of the Repfile-SNV method, when the number of TC and TN standard data was 120, the R_t^2 was the largest, 0.701 and 0.722, respectively, and the RMSEP was 2.880 and 0.399, respectively. After the hyperspectral data were calibration transferred by the above algorithms, they could be predicted by the soil TC and TN concentration model established by using a normal spectrometer, and better prediction results can be obtained. The solution of the calibration transfer of soil nutrient concentration from the hyperspectral camera to the normal spectrometer provides a powerful basis for rapid prediction of a large number of image information data collected by using a hyperspectral camera. It greatly reduces the workload and promotes the application of hyperspectral camera in quantitative analysis and rapid measurement technology.

1. Introduction

The detection technology of soil nutrient concentration by using a normal spectrometer has been relatively mature. The spectral data determined by using the normal spectrometer and the nutrient concentration value of soil samples are used to establish the relevant nutrient concentration model [1–4]. The nutrient concentration of unknown soil samples can be predicted by the model. Before the establishment of the model, pretreatment spectrum and extraction characteristic spectrum are first obtained, so as to achieve better model results [5, 6]. Partial least squares regression is the most

commonly used method for quantitative analysis [7–9]. And some methods such as least squares support vector machine and backpropagation neural network are also used to establish the model of soil nutrient concentration [10–12]. Normally, the more the number of soil samples and the wider the range of soil nutrient concentration, the better the model effect.

Hyperspectral data have spatial and spectral information. Spatial information can represent the morphological characteristics of soil spatial distribution, and spectral information can represent the spectral characteristics of a certain pixel [13–15]. The hyperspectral data acquired by using a hyperspectral camera is displayed in image form. Each pixel has a nearly continuous spectral curve, which is similar to the spectral data acquired by using a normal spectrometer. Hyperspectral camera can obtain a large number of spectral data and spatial data at the same time. It has a certain application in the field of remote sensing classification [16, 17]. Because of the uncertainty of the sample concentration corresponding to the hyperspectral data, the quantitative analysis based on hyperspectral data is mostly limited to the analysis in laboratory [18].

The spectral data of a normal spectrometer are easy to obtain, the corresponding soil nutrient concentration is also easy to determine, and the establishment of soil nutrient concentration model based on spectral technology is mature. A stable soil nutrient concentration model is established with the spectral data collected by using a normal spectrometer. If the hyperspectral data can be transformed into data in some way which is suitable for the established stable soil nutrient concentration model, good prediction results can be obtained. It will play an important role in quantitative analysis of hyperspectral data. This requires calibration transfer algorithm to solve the difference between spectral data of the normal spectrometer and hyperspectral camera.

In the study of calibration transfer using the normal spectrometer, the calibration transfer of different temperatures, different normal spectrometers, and samples from different regions has been studied [19–23]. Some calibration transfer methods are commonly used, such as piecewise direct standardization, direct standardization canonical correlation analysis, and slope/bias correction. However, there are few studies on calibration transfer from the hyperspectral camera to the normal spectrometer.

In this paper, 164 soil samples were collected from Qingdao, China. The spectral data of normal spectrometer and hyperspectral camera and the concentration of total carbon and total nitrogen were obtained. And then, the models of soil total carbon and total nitrogen concentration were established by using the spectral data of a normal spectrometer. The hyperspectral data were transferred by a variety of methods, such as single conventional calibration transfer algorithm, combination of multiple calibration transfer algorithms, and calibration transfer algorithm after spectral pretreatment. The transferred hyperspectral data were predicted by the total carbon and total nitrogen concentration model established by using the normal spectrometer. The absolute coefficients R_t^2 and root mean square error of prediction (RMSEP) were used to evaluate the prediction performance after calibration transfer. By analyzing the prediction performance of various calibration transfer methods, the optimal method was found to realize the calibration transfer of soil nutrient content from the hyperspectral camera to the normal spectrometer.

2. Experimental Section

2.1. Soil Samples. Soil samples were collected from the foot of Fushan Mountain (60 soil samples), the farmland of Zaoshan Mountain (44 soil samples), and the riverside of Licun River (60 soil samples) in Qingdao, China, a total of 164 soil samples. The soil samples of the foot of Fushan Mountain and the farmland of Zaoshan Mountain were sandy loam, and the soil samples of the riverside of Licun River were silty loam. After drying to a constant weight at 55 C, all soil samples were filtered through a 0.45 mm nylon screen and packed in sample bags. Soil TN and TC concentrations of 5–10 g soil sample were measured with a carbon and nitrogen analyzer (Perkin Elemental Analyzer, USA). The statistical table of TC and TN concentrations is shown in Table 1.

2.2. Spectral Data Acquisition. An Ocean Optics QE65000 spectrometer was used as a normal spectromater. The sampling interval was 1 nm, and the spectral range was 200–1100 nm. Soil (3–5 g) was gently flattened in a homemade sample box, whose size was the same as the optical fiber probe bracket. The optical fiber probe was inserted into the hole of the probe bracket at a 45-degree angle, and this made the probe stick to the bracket and just expose the bracket (Figure 1(a)). The spectral reflectance of each soil sample was measured five times, and the average value was obtained. The portable hyperspectral camera GaiaField-V10 was used to obtain hyperspectral images of soil samples. The sampling interval was 3.2 nm, and the spectral range was 400–1100 nm. Soil samples were gently flattened in a rectangular box. The hyperspectral camera was placed on a tripod, and soil samples were taken vertically (Figure 1(b)). Three soil samples were collected from each hyperspectral image.

To reduce the influence of the noise in the reflectance spectrum by the normal spectrometer, the spectral data of 226–975 nm were retained. The reflectance spectrum of all soil samples obtained by the normal spectrometer is shown in Figure 2(a). The image of soil sample was collected by using the hyperspectral camera, and the region of interest (ROI) of the image was extracted by a rectangular figure of $100 * 100$ pixels size. The average spectral value of each point in the ROI region was obtained. The reflectance spectrum of all soil samples by the hyperspectral camera is shown in Figure 2(b). Common spectral bands were obtained between the normal spectrometer and hyperspectral camera, a total of 169 wavelength points. The average spectra of all soil samples under the two instruments were plotted, and the difference was significant (Figure 2(c)).

3. Method

3.1. Calibration, Test, and Standard Data Preparation. One hundred sixty-four soil samples were arranged according to the order of soil samples from the foot of

Table 1: Soil sample TC and TN concentrations.

Soil nutrient	Number	Range	Mean ± SD
TC (mg/kg)	164	1.90–13.40	6.37 ± 3.54
TN (mg/kg)	164	0.21–1.74	0.82 ± 0.48

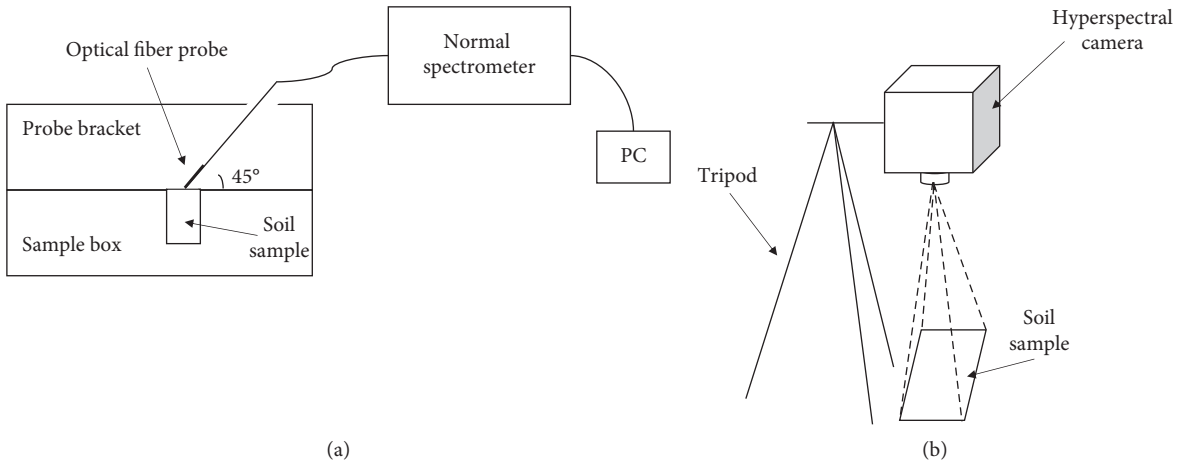

Figure 1: Schematic diagram of soil spectral data measurements. (a) Normal spectrometer; (b) hyperspectral camera.

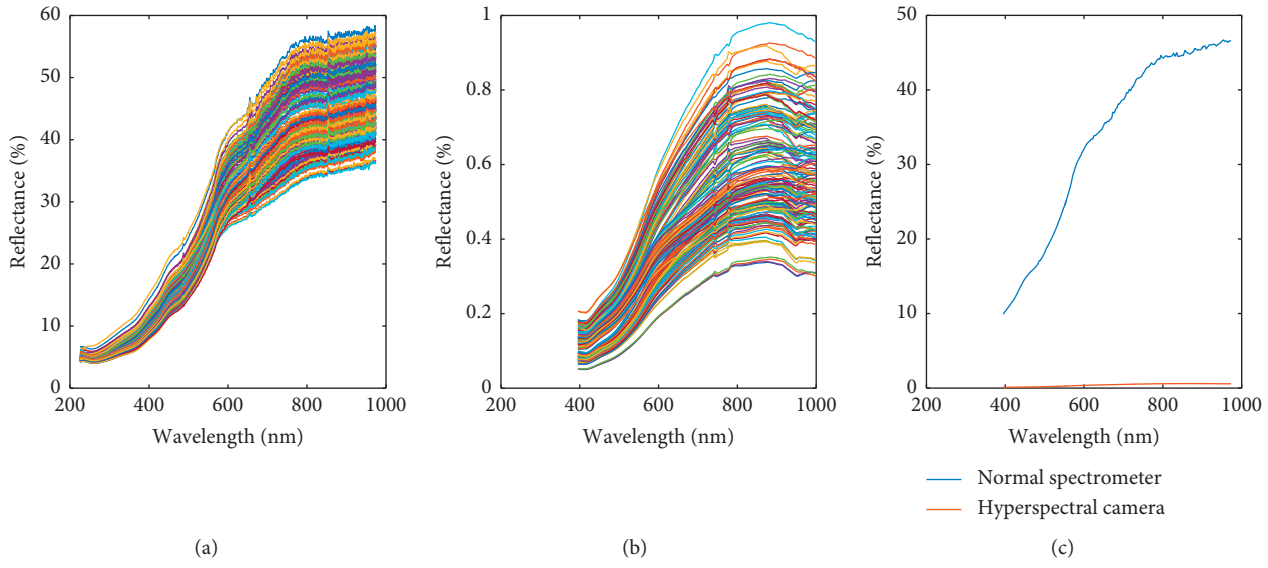

Figure 2: (a) The reflectance spectrum of all soil samples by the normal spectrometer, (b) the reflectance spectrum of all soil samples by the hyperspectral camera, and (c) the average spectra of all soil samples under the two instruments.

Fushan Mountain, the farmland of Zaoshan Mountain, and the riverside of Licun River, and the serial number was marked. In order to ensure that TC and TN concentrations covered by calibration data and test data were wide, the calibration data and test data of normal spectrometer were divided into 3 : 1 proportions by the sequential classification method, with 123 soil samples as the calibration data and 41 soil samples as the test data. The sequential classification method is to classify the samples in proportion according to the sequence of sample numbers. For example, the calibration data and the test data are classified in 3 : 1 proportion by the sequential classification method, and the samples with serial numbers 1, 2, and 3 are taken as the calibration data, and the samples with serial number 4 are taken as the test data.

In the study on the calibration transfer of soil nutrient concentration from the hyperspectral camera to the normal spectrometer, various calibration transfer algorithms are

needed to set up some samples as standard data from the original samples. Some soil samples in the calibration data of the normal spectrometer were used as standard data, and standard data were obtained by sequential classification. The soil samples of the hyperspectral camera, which were consistent with the serial number of the standard data of the normal spectrometer, are used as the standard data of the hyperspectral camera.

3.2. Establishment of the PLSR Model. Partial least squares regression (PLSR) is a common multivariate analysis method for spectral modeling [24, 25]. The method combines principal component analysis with regression analysis. It obtains the principal component matrix of spectral matrix and concentration matrix, respectively. The two matrices are correlated, and their linear relationship is obtained. The established linear relationship is used to predict unknown samples. The advantage of PLSR is that it can fully extract the effective spectral information, fully consider the relationship between spectral matrix and concentration matrix, and ensure the best correction model. The evaluation standard quantitative models are the absolute coefficients R_c^2 and R_p^2 between measured and predicted values of calibration data and test data, root mean square error of calibration (RMSEC), root mean square error of prediction (RMSEP), and residual predictive deviation (RPD). Good models have higher R_c^2, R_p^2, and RPD and smaller RMSEC and RMSEP.

The calibration data and test data of normal spectrometer were divided into 3 : 1 proportions by the sequential classification method. The calibration data were used to establish the correction model of TC and TN concentrations by PLSR, and the test data were used to test the model. The R_c^2 and R_p^2 of TC and TN concentrations were all greater than 0.85, the RPD was both larger than 2.3, and the RMSEC and RMSEP were smaller (Table 2). Therefore, TC and TN concentrations could be used as better quantitative models.

3.3. Calibration Transfer Algorithm. Calibration transfer is usually a method that converts the data of a slave instrument into a stable model applicable to a master instrument. In this paper, the following calibration transfer methods are used to solve the problem of calibration transfer between the normal spectrometer and hyperspectral camera, in which the normal spectrometer is the master instrument and hyperspectral camera is the slave instrument. Calibration transfer methods include model updating, repeatability file model, direct standardization, piecewise direct standardization, canonical correlation analysis, and slope/bias correction. In this paper, X_{oc} and X_{hc} are the spectral data of calibration data by using a normal spectrometer and hyperspectral camera, and their corresponding concentrations are y_{oc} and y_{hc}. X_{ot} and X_{ht} are the spectral data of the test data by using a normal spectrometer and hyperspectral camera, and their corresponding concentrations are y_{ot} and y_{ht}. X_{os} and X_{hs} are the spectral data of the standard data by using a normal spectrometer and hyperspectral camera, and their corresponding concentrations are y_{os} and y_{hs}.

Table 2: Model results of soil sample TC and TN concentrations by the spectral data of the normal spectrometer.

Soil nutrient	R_c^2	RMSEC	R_p^2	RMSEP	RPD
TC	0.861	1.288	0.851	1.602	2.350
TN	0.894	0.152	0.878	0.184	2.741

3.3.1. Model Updating. Model updating is to rebuild the model by adding part of the samples from the slave instrument to the original samples of the main instrument [26, 27]. The specific algorithm is as follows: the spectral data of the standard data by using the slave instrument and its corresponding concentration are added to the calibration data by using the master instrument, that is, (X_{hs}, y_{hs}), is added to (X_{oc}, y_{oc}). And then, the new sample concentration model is reestablished by PLSR. By adding spectral data X_{ht} of the test data by the slave instrument to the new model for calculation, the predicted concentration of this can be obtained.

3.3.2. Repeatability File Model. Repeatability file model (Repfile model) is to rebuild the model by adding the difference spectrum of the standard data by the master instrument and slave instrument and their corresponding concentration difference in the concentration model of the original samples [28, 29]. The specific algorithm is as follows: calculate the difference spectrum of the standard data by master instrument and slave instrument, $D = X_{os} - X_{hs}$, and set the corresponding concentration difference y_d to zero. (D, y_d) is added to (X_{oc}, y_{oc}). And then, the new sample concentration model is reestablished by PLSR. By adding spectral data X_{ht} of the test data by the slave instrument to the new model for calculation, the predicted concentration of this can be obtained.

3.3.3. Direct Standardization and Piecewise Direct Standardization. Direct standardization (DS) and piecewise direct standardization (PDS) both realized the calibration transfer by constructing the relationship between the spectrum of the master and the slave instrument. First, the relationship between the standard data of the master and the slave instrument is calculated, and the transfer matrix is obtained. Then, adding spectral data of the test data by the slave instrument to the relation for calculation, a new spectrum which is similar to the spectrum of the master instrument is obtained. Finally, the new spectrum to the model of the master instrument is added for prediction. The specific algorithm of DS is as follows [30, 31]: calculate the transfer matrix, $F = (X_{hs}' X_{hs})^{-1} X_{hs}' X_{os}$. The new spectrum is calculated according to the transfer matrix, $X_{htF} = X_{ht} \cdot F$.

PDS is based on DS, which adds a dynamic window. The specific algorithm is as follows [32, 33]: the spectral band of the window width $(j - k \sim j + k)$ is intercepted near the jth wavelength point; let $Z_j = [X_{hs,j-k}, \ldots, X_{hs,j}, X_{hs,j+1}, \ldots X_{hs,j+k}]$. Construct the multiple linear regression equation between $X_{hs,j}$ and Z_j, $X_{os,j} = Z_j \times f_j + e_j$. And then, the regression coefficients f_j are calculated by PLSR. Loop j, and find all the f_j. Put f_j on the main diagonal of

the transformation matrix F, set other elements as zero, and finally get the transformation matrix F. The new spectrum is calculated according to the transfer matrix, $X_{htF} = X_{ht} \cdot F$.

3.3.4. Canonical Correlation Analysis. The principle of canonical correlation analysis (CCA) is to find a linear combination (canonical correlation coefficient) w_m and w_s, according to the spectral data X_{os} and X_{hs} of standard by the master and slave instrument [21, 34]. And then, make the correlation coefficient of $X_{os} \times w_m$ and $X_{hs} \times w_s$ maximum, the product results become canonical correlation components. The specific algorithm is as follows: according to $X_{os}$and X_{hs} calculate matrix $C = \begin{bmatrix} X_{os}^t X_{os} & X_{os}^t X_{hs} \\ X_{hs}^t X_{os} & X_{hs}^t X_{hs} \end{bmatrix} = \begin{bmatrix} C_{aa} & C_{ab} \\ C_{ba} & C_{bb} \end{bmatrix}$, calculate the eigenvalues and eigenvectors $\begin{cases} C_{aa}^{-1} C_{ab} C_{bb}^{-1} C_{ba} w_m = \rho^2 w_m \\ C_{bb}^{-1} C_{ba} C_{aa}^{-1} C_{ab} w_s = \rho^2 w_s \end{cases}$. All the eigenvectors w_m and w_s corresponding to each nonzero eigenvalue ρ are classified into matrix W_m and W_s, respectively. W_m and W_s are the canonical correlation coefficients of X_{os} and X_{hs}. X_{os} and X_{hs} are decomposed by CCA, and the canonical correlation components L_m and L_S of X_{os} and X_{hs} are calculated. Finally, the transfer matrix F is obtained. The formula is as follows: $L_m = X_{os} \times W_m$, $L_S = X_{hs} \times W_s$, $F_1 = L_S^{t+} \times L_m$, $F_2 = L_m^{t+} \times X_{os}$, and $F = W_s \times F_1 \times F_2$. The new spectrum is calculated according to the transfer matrix, $X_{htF} = X_{ht} \cdot F$.

3.3.5. Slope/Bias Correction. Slope/bias correction (SBC) is based on the sample concentration model established by the master instrument, the spectral data of the standard data by the slave instrument to the model are added and the concentration y_{hsp} of the standard data by the slave instrument is predicted [35, 36]. A linear regression equation is used to fit the measured concentration y_{hs} and the predicted concentration y_{hsp} of the standard data by the slave instrument. According to the formula $y_{hs} = s \cdot y_{hsp} + b$, the least square solution of the linear equation is obtained, that is, slope s and bias b of the linear model. By adding the spectral data of the test data by the slave instrument to the concentration model of the master instrument, the concentration of the test data by the slave instrument can be predicted. The final concentration prediction value of the test data by the slave instrument can be obtained according to the calculated slope s and bias b.

3.4. Evaluation Standard of Prediction Performance. The evaluation standard of prediction performance is the absolute coefficients R_t^2 and root mean square error of prediction (RMSEP). The closer the R_t^2 is to 1 and the smaller the RMSEP is, the better the prediction performance is. The calculation formula is as follows:

$$R_t^2 = 1 - \frac{\sum_{i=1}^{n} (y_i - \hat{y}_i)^2}{\sum_{i=1}^{n} (y_i - \overline{y})^2},$$
$$\text{RMSEP} = \sqrt{\frac{\sum_{i=1}^{n} (y_i - \hat{y}_i)}{n}}, \quad (1)$$

where n is the number of the test data by the slave instrument, y_i is the ith sample's measured concentration of the test data by the slave instrument, $\hat{y}_i$ is the ith sample's predicted concentration of the test data by the slave instrument after calibration transfer, and $\overline{y}$ is all sample's mean concentration of the test data by the slave instrument.

4. Results and Discussion

A variety of calibration transfer algorithms were used to study the calibration transfer of soil nutrient concentration from the hyperspectral camera to the normal spectrometer. On the basis of various calibration transfer algorithms, the spectral data were preprocessed by standard normal variate, and then, the calibration transfer was carried out. According to the prediction results of each calibration transfer algorithm, the optimal calibration transfer algorithm for soil TC and TN concentrations from hyperspectral camera to normal spectrometer was analyzed.

4.1. Prediction Results of Single Calibration Transfer Algorithm. Six calibration transfer algorithms (model updating, Repfile model, DS, PDS, CCA, and SBC) were used to calibration transfer from hyperspectral cameras to normal spectrometers, respectively. The R_t^2 and RMSEP values of soil TC and TN concentrations are shown in Table 3. The number of PDS window was 19, and the number of standard data was 30.

Single calibration transfer algorithm could not improve the prediction performance of soil TC and TN concentrations. In the prediction results of TC concentration, the R_t^2 values of calibration transfer algorithms were all smaller than those without calibration transfer. Except for PDS, the RMSEP values of other calibration transfer algorithms were slightly lower than those without calibration transfer. In the prediction results of TN concentration, except for PDS, the R_t^2 values of other calibration transfer algorithms were all not less than those without calibration transfer, and the RMSEP values were all less than those without calibration transfer.

4.2. Prediction Results of the Repfile Model Combined with PDS. Model updating and Repfile model belong to the calibration transfer method for reestablishing the model. DS, PDS, and CCA belong to the calibration transfer method for correcting spectral data. SBC belongs to calibration transfer method for correcting concentration value. In reestablishing model methods, the prediction results of TC and TN concentration by the Repfile model are better than those by model updating. Among the three methods for correcting

Table 3: Prediction results of soil TC and TN concentration by different calibration transfer algorithms.

Calibration transfer methods	TC		TN	
	R_t^2	RMSEP	R_t^2	RMSEP
None	0.307	14.907	0.187	2.226
Model updating	0.276	3.715	0.246	0.498
Repfile model	0.286	11.486	0.271	1.475
PDS	0.243	38.051	0.141	5.449
DS	0.251	5.101	0.330	0.605
CCA	0.143	6.752	0.222	0.779
SBC	0.307	3.120	0.187	0.258

spectral data, PDS has the greatest plasticity and can change the prediction performance by changing the window. The method for correcting concentration values can only change the predicted concentration values but cannot improve R_t^2. Therefore, the Repfile model combined with PDS (Repfile-PDS) is used for studying calibration transfer from the hyperspectral camera to normal spectrometer.

When the number of PDS window was 19 and the number of standard data was 30, the prediction results of TC and TN concentrations by Repfile-PDS were obtained. The R_t^2 values of TC and TN were 0.611 and 0.648, and the RMSEP values of TC and TN were 2.376 and 0.301, respectively. Compared with single calibration transfer algorithm, the prediction results were improved significantly.

The number of PDS windows and the number of standard data had different effects on the prediction performance of TC and TN concentrations. First, the number of PDS window was determined. The PDS window ranged from 3 to 27, and the interval was 2. The R_t^2 values of TC and TN concentrations with different PDS window widths by Repfile-PDS are shown in Figure 3, and the number of standard data was set as 30. When the number of PDS windows was 27 and 25, the R_t^2 values of TC and TN concentrations were the largest. In the following study, the number of PDS windows of TC and TN was set to 27 and 25.

Under the condition that the number of PDS windows of TC and TN was 27 and 25, the different effects of the number of standard data on the prediction results of TC and TN concentrations were studied. The number of the standard data ranged from 10 to 120 by sequential classification, and the interval was 10. The prediction results of TC and TN concentration by Repfile-PDS are shown in Table 4.

Table 4 shows that when the number of TC and TN standard data was 40 and 100, respectively, the R_t^2 values were the largest, 0.627 and 0.666, respectively, and the RMSEP values were the smallest, 2.351 and 0.297, respectively. In the prediction results of TC concentration, when the number of standard data was 20–120, R_t^2 was about 0.6, and the RMSEP value was about 2.5. When the number of standard data was 10, the prediction results were bad. In the prediction results of TN concentration, when the number of standard data was 10, 20, 50, and 70, they had bad performance. In the case of the number of samples in other standard data, R_t^2 was about 0.6 and the RMSEP value was below 0.32. When the number of standard data reached a

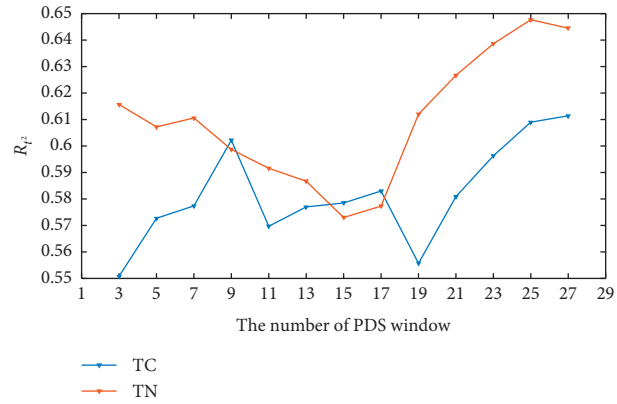

Figure 3: R_t^2 of soil TC and TN concentration with different PDS window widths by Repfile-PDS.

Table 4: Prediction results of TC and TN concentrations with different numbers of standard data by Repfile-PDS.

The number of standard set	TC		TN	
	R_t^2	RMSEP	R_t^2	RMSEP
10	0.336	4.020	0.428	0.495
20	0.608	2.687	0.293	0.440
30	0.611	2.376	0.648	0.301
40	0.627	2.351	0.632	0.313
50	0.577	2.521	0.438	0.381
60	0.603	2.436	0.627	0.315
70	0.563	2.534	0.586	0.327
80	0.624	2.508	0.630	0.324
90	0.616	2.426	0.636	0.311
100	0.615	2.399	0.666	0.297
110	0.596	2.477	0.618	0.319
120	0.604	2.441	0.627	0.314

certain number, different number of standard data had less influence on the prediction effect by Repfile-PDS.

4.3. Prediction Results of Single Calibration Transfer Algorithm Combined with SNV. Standard normal variate (SNV) is the difference between the original spectrum and the average of the spectrum and is then divided by the standard deviation of the spectral data. The essence of SNV is to make the original spectral data standard normalization. Its function is to eliminate the influence of solid particle size, surface scattering, and optical path change on the spectrum [37, 38].

Without SNV spectral pretreatment, the spectral data of the normal spectrometer and hyperspectral camera for soil samples with poor and rich nutrient concentration were quite different (Figures 4(a) and 4(c)). However, the difference between the two spectra became smaller by SNV spectral pretreatment, and the general trend of spectral curse was the same (Figures 4(b) and 4(d)). Subsequently, the calibration transfer methods of spectral data pretreated by SNV would be studied.

After SNV spectral pretreatment, six calibration transfer algorithms, namely, model updating, Repfile model, DS, PDS, CCA, and SBC, were used to transfer the model

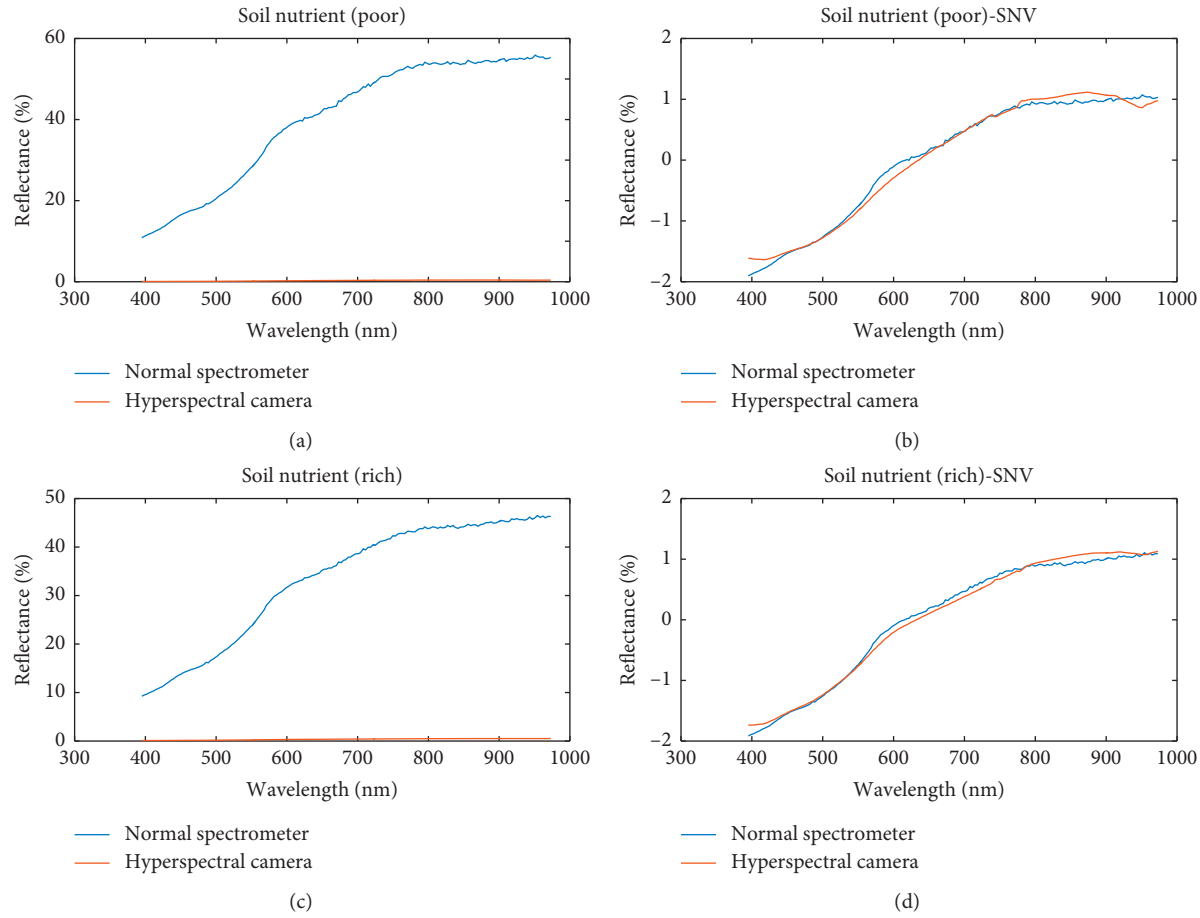

Figure 4: The spectral data of normal spectrometer and hyperspectral camera for soil samples (a) with poor nutrient concentration (TC: 1.9 mg/kg; TN: 0.21 mg/kg), (b) with poor nutrient concentration by SNV, (c) with rich nutrient content (TC: 12.19 mg/kg; TN: 1.74 mg/kg), and (d) with poor and rich nutrient concentration by SNV.

between the hyperspectral camera and normal spectrometer. The R_t^2 and RMSEP values of soil TC and TN concentration prediction results are shown in Table 5. The number of PDS window was 19, and the number of the standard data was 30.

Table 5 shows that the prediction results are bad after SNV pretreatment, and the prediction results of PDS, DS, CCA, and SBC calibration transfer algorithms after SNV pretreatment were not significantly improved. The Repfile model and model updating were spectrally pretreated by SNV, and the prediction results of the Repfile model were better. The R_t^2 values of TC and TN were 0.587 and 0.618, respectively, and the RMSEP values were 3.437 and 0.418, respectively. Therefore, SNV combined with the Repfile model could improve the prediction performance of soil nutrient concentration from the hyperspectral camera to the normal spectrometer.

4.4. Prediction Results of the Repfile Model Combined with SNV. In order to further study the prediction results on TC and TN content prediction in different numbers of standard data by Repfile model combined with SNV (Repfile-SNV), the number of the standard data ranged from 10 to 120 by sequential classification, and the interval was 10. The prediction results of TC and TN concentrations by Repfile-SNV are shown in Table 6.

Table 5: Prediction results of soil TC and TN concentration by different calibration transfer algorithms after SNV spectral pretreatment.

Calibration transfer methods	TC		TN	
	R_t^2	RMSEP	R_t^2	RMSEP
None	0.199	9.409	0.220	1.251
Repfile model	0.587	3.437	0.618	0.418
Model updating	0.474	2.816	0.537	0.352
PDS	0.046	108.395	0.017	13.120
DS	0.263	4.290	0.210	0.622
CCA	0.238	4.647	0.179	0.683
SBC	0.199	3.465	0.187	0.454

Table 6 shows that when the number of TC and TN standard data is 120, R_t^2 was the largest, 0.701 and 0.722, respectively, and the RMSEP value is 2.880 and 0.399, respectively. In the prediction results of TC concentration, when the number of standard sets was not less than 40, the R_t^2 was greater than 0.6. In the prediction results of TN concentration, when the number of the standard sets was not less than 20, the R_t^2 value was greater than 0.6. The R_t^2 of TC

Table 6: Prediction results of TC and TN concentration with different numbers of standard data by Repfile-SNV.

The number of standard set	TC		TN	
	R_t^2	RMSEP	R_t^2	RMSEP
10	0.520	2.960	0.546	0.374
20	0.588	2.611	0.617	0.315
30	0.587	3.437	0.618	0.418
40	0.628	2.332	0.649	0.311
50	0.621	3.306	0.635	0.312
60	0.606	2.516	0.630	0.314
70	0.601	3.042	0.623	0.308
80	0.695	2.092	0.720	0.278
90	0.694	2.408	0.711	0.269
100	0.635	3.620	0.656	0.428
110	0.697	3.055	0.722	0.424
120	0.701	2.880	0.722	0.399

and TN approximately increased with the number of standard data.

4.5. Discussion

4.5.1. Differentiation between Calibration Transfer in This Paper and Other Calibration Transfer. The calibration transfer in this paper is to solve the problem of calibration transfer between the hyperspectral camera and the normal spectrometer, which is essentially a calibration transfer between instruments. However, compared with the calibration transfer between normal spectrometers, the calibration transfer between the hyperspectral camera and the normal spectrometer is more difficult. The data obtained by a hyperspectral camera show an image, and the image data should be processed and analyzed. Hyperspectral cameras are mostly used for the field to acquire data. Not only are there differences between instruments, but also the spectral information of the same sample will be different due to illumination, environment, and other factors, which brings great difficulties to the calibration transfer between hyperspectral cameras and normal spectrometers. Figures 2(c), 4(a), and 4(c) show that the spectral data of hyperspectral cameras are quite different from those of normal spectrometers. The conventional calibration transfer algorithm alone cannot solve the problem of calibration transfer. PDS, DS, and CCA are three kinds of conventional calibration transfer algorithms, which belong to the calibration transfer method of correcting spectral data. The transfer matrix is calculated from the spectral data of two standard data of instruments to realize calibration transfer. Due to the influence of instruments, external environment, and other factors, the spectral data between the normal spectrometer and hyperspectral camera are quite different. So the calibration transfer based on the transfer matrix alone cannot achieve better prediction results.

4.5.2. Analysis between Repfile-PDS and Repfile-SNV. The Repfile-PDS and Repfile-SNV methods have the best prediction performance after trying many calibration transfer algorithms. The SNV method eliminates the influence of solid particle size, surface scattering, and optical path change between the hyperspectral camera and normal spectrometer. The PDS method carries out preliminary calibration transfer of spectral data between the hyperspectral camera and normal spectrometer instrument by the transfer matrix. Both the SNV and PDS methods reduce the differences between the two instruments in spectral data. The Repfile model method is to reestablish the model by adding the difference spectrum between the hyperspectral camera and normal spectrometer and to introduce the difference between the two into the new model. The SNV and PDS methods are, respectively, combined with the Repfile model method to solve the calibration transfer problem between the hyperspectral camera and normal spectrometer, and good prediction results are obtained. The Repfile-SNV method is slightly better than the Repfile-PDS. Especially when the number of standard data increases, the performance is more obvious. Therefore, the SNV method is superior to the PDS method in eliminating spectral differences between the two instruments.

Table 7: Model results of soil samples TC and TN concentration by the spectral data of the hyperspectral camera.

Soil nutrient	R_c^2	RMSEC	R_p^2	RMSEP	RPD
TC	0.626	2.114	0.728	2.106	1.788
TN	0.708	0.252	0.808	0.238	2.119

The calibration models of TC and TN concentrations in soil spectral data obtained from 164 hyperspectral camera data were established by PLSR. The calibration data and test data of hyperspectral camera were divided into 3 : 1 proportions by the sequential classification method. The prediction results are shown in Table 7. The test data of hyperspectral TC and TN concentration models are the same as those by calibration transfer algorithm. The best prediction results of calibration transfer are obtained using the Repfile-SNV method, the R_t^2 values for TC and TN are 0.701 and 0.722, and the RMSEP values are 2.880 and 0.399. The R_t^2 values of soil TC and TN concentration by the spectral data of hyperspectral camera are 0.728 and 0.808, and the RMSEP values are 2.106 and 0.238. The optimal prediction results by the Repfile-SNV method are close to the TC and TN prediction results of hyperspectral data self-modeling. Therefore, the Repfile-SNV method is a feasible method of calibration transfer from the hyperspectral camera to the normal spectrometer in soil nutrient concentration.

4.5.3. Future Research. The hyperspectral data collected by the hyperspectral camera in this paper are still collected indoors and are not real-field hyperspectral data. In the future, field hyperspectral data will be collected to study the calibration transfer of soil nutrient concentration from the hyperspectral camera to normal spectrometer. The number of standard data still has some influence on the effect of calibration transfer methods. In the future, it is hoped that the problem of calibration transfer of soil nutrient concentration from the hyperspectral camera to normal

spectrometer can be solved without the influence of the number of the standard data or a small number of the standard data.

5. Conclusions

The calibration transfer between instruments is mainly aimed at the calibration transfer between normal spectrometers. There are few studies on the calibration transfer of soil nutrient concentration from a hyperspectral camera to a normal spectrometer. In this paper, 164 soil samples from three regions in Qingdao, China, were collected. The spectral data of normal spectrometer and hyperspectral camera and the concentration of total carbon and total nitrogen were obtained. And then, the models of soil total carbon and total nitrogen content were established by using the spectral data of a normal spectrometer. The hyperspectral data were transferred by a variety of methods, such as single conventional calibration transfer algorithm, combination of multiple calibration transfer algorithms, and calibration transfer algorithm after spectral pretreatment. The transferred hyperspectral data were predicted by the total carbon and total nitrogen concentration model established by the normal spectrometer. The absolute coefficients R_t^2 and root mean square error of prediction RMSEP were used to evaluate the prediction performance after calibration transfer. After trying many calibration transfer methods, the prediction performance of calibration transfer by the Repfile-PDS and Repfile-SNV method was the best. In the calibration transfer of the Repfile-PDS method, when the number of PDS windows was 27 and the number of standard data was 40, the R_t^2 and the RMSEP of TC concentration were 0.627 and 2.351. When the number of PDS windows was 25 and the number of standard data was 100, the R_t^2 and the RMSEP of TN concentration were 0.666 and 0.297. In the calibration transfer of the Repfile-SNV method, when the number of TC and TN standard data was 120, the R_t^2 were the largest, 0.701 and 0.722, respectively, and the RMSEP were 2.880 and 0.399, respectively. After the hyperspectral data were calibration transferred by the above algorithms, they could be predicted by the soil TC and TN concentration model established by using a normal spectrometer, and better prediction results can be obtained. The solution of the calibration transfer of soil nutrient concentration from the hyperspectral camera to the normal spectrometer provides a powerful basis for rapid prediction of a large number of image information data collected by using a hyperspectral camera. It greatly reduces the workload and promotes the application of hyperspectral camera in quantitative analysis and rapid measurement technology.

Data Availability

All data in the paper are fully available without restriction at https://figshare.com/s/6c301c6479dc3f1a554c or from the corresponding author upon request.

Conflicts of Interest

The authors declare that there are no conflicts of interest.

Acknowledgments

This work was supported by the Shandong Provincial Natural Science Foundation, China (Nos. ZR2018LD007, ZR2017BB037, and ZR2019PD004), the Natural Science Foundation of Shandong Province, China (No. ZR2018ZB0532), and the National Natural Science Foundation of China (No. 31700447).

References

[1] F. Feyziyev, M. Babayev, S. Priori, and G. L'Abate, "Using visible-near infrared spectroscopy to predict soil properties of mugan plain, Azerbaijan," *Open Journal of Soil Science*, vol. 6, no. 3, pp. 52–58, 2016.

[2] M. Paradelo, C. Hermansen, M. Knadel, P. Moldrup, M. H. Greve, and L. W. de Jonge, "Field-scale predictions of soil contaminant sorption using visible-near infrared spectroscopy," *Journal of Near Infrared Spectroscopy*, vol. 24, no. 3, pp. 281–291, 2016.

[3] A. M. Mouazen and B. Kuang, "On-line visible and near infrared spectroscopy for in-field phosphorous management," *Soil and Tillage Research*, vol. 155, pp. 471–477, 2016.

[4] D. Cozzolino, "Near infrared spectroscopy as a tool to monitor contaminants in soil, sediments and water-State of the art, advantages and pitfalls," *Trends in Environmental Analytical Chemistry*, vol. 9, no. 2, pp. 1–7, 2016.

[5] T. Pan, Y. Han, J. Chen, L. Yao, and J. Xie, "Optimal partner wavelength combination method with application to near-infrared spectroscopic analysis," *Chemometrics and Intelligent Laboratory Systems*, vol. 156, pp. 217–223, 2016.

[6] K. Kensuke, T. Yasuhiro, R. Michel et al., "Vis-NIR spectroscopy and PLS regression with waveband selection for estimating the total C and N of paddy soils in Madagascar," *Remote Sensing*, vol. 9, no. 10, p. 1081, 2017.

[7] X. Yu, Q. Liu, Y. Wang, X. Liu, and X. Liu, "Evaluation of MLSR and PLSR for estimating soil element contents using visible/near-infrared spectroscopy in apple orchards on the Jiaodong peninsula," *Catena*, vol. 137, pp. 340–349, 2016.

[8] N. K. Niazi, B. Singh, and B. Minasny, "Mid-infrared spectroscopy and partial least-squares regression to estimate soil arsenic at a highly variable arsenic-contaminated site," *International Journal of Environmental Science & Technology*, vol. 12, no. 6, pp. 1–10, 2015.

[9] L. J. Janik, S. T. Forrester, and A. Rawson, "The prediction of soil chemical and physical properties from mid-infrared spectroscopy and combined partial least-squares regression and neural networks (PLS-NN) analysis," *Chemometrics and Intelligent Laboratory Systems*, vol. 97, no. 2, pp. 179–188, 2009.

[10] N. Pengcheng, D. Tao, H. Yong et al., "Detection of soil nitrogen using near infrared sensors based on soil pretreatment and algorithm," *Sensors*, vol. 17, no. 5, p. 1102, 2017.

[11] A. Morellos, X.-E. Pantazi, D. Alexandridis et al., "Machine learning based prediction of soil total nitrogen, organic carbon and moisture content by using VIS-NIR spectroscopy," *Biosystems Engineering*, vol. 152, pp. 104–116, 2016.

[12] S. Xu, M. Y. Zhao, and X. Shi, "Comparison of multivariate methods for estimating selected soil properties from intact soil cores of paddy fields by Vis-NIR spectroscopy," *Geoderma*, vol. 310, pp. 29–43, 2018.

[13] J. Shengyao, L. Hongyang, W. Yanjie et al., "Hyperspectral imaging analysis for the classification of soil types and the

determination of soil total nitrogen," *Sensors*, vol. 17, no. 10, p. 2252, 2017.

[14] K. Bhardwaj and S. Patra, "An unsupervised technique for optimal feature selection in attribute profiles for spectral-spatial classification of hyperspectral images," *ISPRS Journal of Photogrammetry and Remote Sensing*, vol. 138, pp. 139–150, 2018.

[15] J. M. Haut, M. Paoletti, and A. J. Plaza, "Cloud implementation of the K-means algorithm for hyperspectral image analysis," *The Journal of Supercomputing*, vol. 73, no. 1, pp. 514–529, 2017.

[16] C. Mccann, K. S. Repasky, M. Morin, R. L. Lawrence, and S. Powell, "Novel histogram based unsupervised classification technique to determine natural classes from biophysically relevant fit parameters to hyperspectral data," *IEEE Journal of Selected Topics in Applied Earth Observations and Remote Sensing*, vol. 10, no. 9, pp. 4138–4148, 2017.

[17] M. Pedergnana, P. R. Marpu, M. D. Mura, J. A. Benediktsson, and L. Bruzzone, "A novel technique for optimal feature selection in attribute profiles based on genetic algorithms," *IEEE Transactions on Geoscience and Remote Sensing*, vol. 51, no. 6, pp. 3514–3528, 2013.

[18] H. Eleanor, S. Markus, L. B. Sara et al., "Hotspots of soil organic carbon storage revealed by laboratory hyperspectral imaging," *Scientific Reports*, vol. 8, Article ID 13900, 2018.

[19] S. Guo, R. Heinke, S. Stöckel, P. Rösch, T. Bocklitz, and J. Popp, "Towards an improvement of model transferability for Raman spectroscopy in biological applications," *Vibrational Spectroscopy*, vol. 91, pp. 111–118, 2017.

[20] S. V. Sanghavi, J. V. Martonchik, A. B. Davis, and D. J. Diner, "Linearization of a scalar matrix operator method radiative transfer model with respect to aerosol and surface properties," *Journal of Quantitative Spectroscopy and Radiative Transfer*, vol. 116, no. 2, pp. 1–16, 2013.

[21] J. Bin, X. Li, W. Fan, J.-h. Zhou, and C.-w. Wang, "Calibration transfer of near-infrared spectroscopy by canonical correlation analysis coupled with wavelet transform," *The Analyst*, vol. 142, no. 12, pp. 2229–2238, 2017.

[22] J. B. Cooper, C. M. Larkin, and M. F. Abdelkader, "Calibration transfer of near-IR partial least squares property models of fuels using virtual standards," *Journal of Chemometrics*, vol. 25, no. 9, pp. 496–505, 2011.

[23] X.-Y. Li, Y. Liu, M.-R. Lv, Y. Zou, and P.-P. Fan, "Calibration transfer of soil total carbon and total nitrogen between two different types of soils based on visible-near-infrared reflectance spectroscopy," *Journal of Spectroscopy*, vol. 2018, Article ID 8513215, 10 pages, 2018.

[24] Q. Chen, J. Zhao, M. Liu, J. Cai, and J. Liu, "Determination of total polyphenols content in green tea using FT-NIR spectroscopy and different PLS algorithms," *Journal of Pharmaceutical and Biomedical Analysis*, vol. 46, no. 3, pp. 568–573, 2008.

[25] Z. Yang, M. Zhang, K. Li et al., "Rapid detection of knot defects on wood surface by near infrared spectroscopy coupled with partial least squares discriminant analysis," *Bioresources*, vol. 11, no. 1, pp. 2557–2567, 2016.

[26] R. N. Feudale, N. A. Woody, H. Tan, A. J. Myles, S. D. Brown, and J. Ferré, "Transfer of multivariate calibration models: a review," *Chemometrics and Intelligent Laboratory Systems*, vol. 64, no. 2, pp. 181–192, 2002.

[27] K. D. Shepherd and M. G. Walsh, "Development of reflectance spectral libraries for characterization of soil properties," *Soil Science Society of America Journal*, vol. 66, no. 3, pp. 988–998, 2002.

[28] J. S. Shenk and M. O. Westerhaus, "New standardization and calibration procedures for nirs analytical systems," *Crop Science*, vol. 31, no. 6, pp. 1694–1696, 1991.

[29] M. Nouri, C. Gomez, N. Gorretta, and J. M. Roger, "Clay content mapping from airborne hyperspectral Vis-NIR data by transferring a laboratory regression model," *Geoderma*, vol. 298, pp. 54–66, 2017.

[30] J.-X. Wang, J. Qu, H. Li, X. Han, and G. Xu, "Application of GA-DS to calibration transfer of aviation fuel density in near infrared spectroscopy," *Petroleum Science and Technology*, vol. 30, no. 19, pp. 1975–1980, 2012.

[31] W. Ji, S. Li, S. Chen, Z. Shi, R. A. Viscarra Rossel, and A. M Mouazen, "Prediction of soil attributes using the Chinese soil spectral library and standardized spectra recorded at field conditions," *Soil and Tillage Research*, vol. 155, pp. 492–500, 2016.

[32] M. Blanco, M. J. Cruz, and M. Armengol, "Control production of polyester resins by NIR spectroscopy," *Microchemical Journal*, vol. 90, no. 2, pp. 118–123, 2008.

[33] C. F. Pereira, M. F. Pimentel, R. K. H. Galvão, F. A. Honorato, L. Stragevitch, and M. N. Martins, "A comparative study of calibration transfer methods for determination of gasoline quality parameters in three different near infrared spectrometers," *Analytica Chimica Acta*, vol. 611, no. 1, pp. 41–47, 2008.

[34] W. Fan, Y. Liang, D. Yuan, and J. Wang, "Calibration model transfer for near-infrared spectra based on canonical correlation analysis," *Analytica Chimica Acta*, vol. 623, no. 1, pp. 22–29, 2008.

[35] D. Abookasis and J. J. Workman, "Direct measurements of blood glucose concentration in the presence of saccharide interferences using slope and bias orthogonal signal correction and Fourier transform near-infrared spectroscopy," *Journal of Biomedical Optics*, vol. 16, no. 2, Article ID 027001, 2011.

[36] J. B. Cooper, C. M. Larkin, and M. F. Abdelkader, "Virtual standard slope and bias calibration transfer of partial least squares jet fuel property models to multiple near infrared spectroscopy instruments," *Journal of Near Infrared Spectroscopy*, vol. 19, no. 2, pp. 139–150, 2011.

[37] T. Fearn, A. C. Riccioli, and J. E. Guerrero-Ginel, "On the geometry of SNV and MSC," *Chemometrics and Intelligent Laboratory Systems*, vol. 96, no. 1, pp. 22–26, 2009.

[38] D. Cozzolino, M. J. Kwiatkowski, R. G. Cynkar et al., "Analysis of elements in wine using near infrared spectroscopy and partial least squares regression," *Talanta*, vol. 74, no. 4, pp. 711–716, 2008.